Cite as: M. Piwecka *et al.*, *Science* 10.1126/science.aam8526 (2017).

Loss of a mammalian circular RNA locus causes miRNA deregulation and affects brain function

Monika Piwecka,[1]* Petar Glažar,[1]* Luis R. Hernandez-Miranda,[2]* Sebastian Memczak,[1,3] Susanne A. Wolf,[4] Agnieszka Rybak-Wolf,[1] Andrei Filipchyk,[1] Filippos Klironomos,[1] Cledi Alicia Cerda Jara,[1] Pascal Fenske,[5] Thorsten Trimbuch,[5] Vera Zywitza,[1] Mireya Plass,[1] Luisa Schreyer,[1] Salah Ayoub,[1] Christine Kocks,[1] Ralf Kühn,[6,7] Christian Rosenmund,[5] Carmen Birchmeier,[2] Nikolaus Rajewsky[1]†

[1]Laboratory for Systems Biology of Gene Regulatory Elements, Berlin Institute for Medical Systems Biology, Max Delbrück Center for Molecular Medicine, Robert-Rössle-Str. 10, Berlin-Buch, Germany. [2]Laboratory for Developmental Biology and Signal Transduction, Max Delbrück Center for Molecular Medicine, Robert-Rössle-Str. 10, Berlin-Buch, Germany. [3]Experimental and Clinical Research Center, a joint cooperation between the Charité Medical Faculty and the Max Delbrück Center for Molecular Medicine, Berlin, Germany. [4]Laboratory for Cellular Neurosciences, Max Delbrück Center for Molecular Medicine, Robert-Rössle-Str. 10, Berlin-Buch, Germany. [5]Department of Neurophysiology, NeuroCure Cluster of Excellence, Charité-Universitätsmedizin, Berlin, Germany. [6]Transgenic Core Facility, Max Delbrück Center for Molecular Medicine, Robert-Rössle-Str. 10, Berlin-Buch, Germany. [7]Berlin Institute of Health, Kapelle-Ufer 2, Berlin, Germany.

*These authors contributed equally to this work.

†Corresponding author. Email: rajewsky@mdc-berlin.de

Hundreds of circular RNAs (circRNAs) are highly abundant in mammalian brain, with oftentimes conserved expression. Here, we show that the circRNA Cdr1as is massively bound by miR-7 and miR-671 in the human and mouse brain. When the *Cdr1as* locus was removed from the mouse genome, knockout animals displayed impaired sensorimotor gating, a deficit in the ability to filter out unnecessary information associated with neuropsychiatric disorders. Electrophysiological recordings revealed dysfunctional synaptic transmission. Expression of microRNAs miR-7 and miR-671 was specifically and post-transcriptionally misregulated in all brain regions analyzed. Expression of immediate early genes such as *Fos*, a direct miR-7 target, was enhanced in *Cdr1as*-deficient brains, providing a possible molecular link to the behavioral phenotype. Our data indicate an in vivo loss-of-function circRNA phenotype and suggest that interactions between circRNAs and miRNAs are important for normal brain function.

In recent years it has been shown that animals express large numbers of single stranded RNA molecules, which are covalently closed at the 5′ and 3′ end (circRNAs) (*1*–*3*). All mammalian circRNAs studied to date are consequences of "backsplicing" in which the spliceosome joins the 3′ end of an exon with an upstream 5′ end of the same or different exons from the same transcript (*4*–*6*). Backsplicing is context dependent (*4*, *7*) and circRNAs are often tissue- and developmental stage-specifically expressed (*3*). In mammals, a few hundred circRNAs are highly expressed in major brain areas, with frequently conserved expression between human and mouse (*7*). In neurons, circRNAs are expressed in the soma and in neurites and have the overall highest concentration at synaptosomes (*7*, *8*). Probably due to the absence of 5′ and 3′ ends, circRNAs feature half lifetimes ranging from hours to days or longer and are therefore generally much more stable than linear coding or noncoding messages (*3*). Thus, circRNAs may carry out biological functions that are different compared to other classes of RNAs, however their normal functions are largely unknown.

Cdr1as is a circularized long noncoding (lnc) RNA that is highly abundant in mammalian brain and expressed at low levels or absent in other tissues and organs. It is highly conserved across mammals and not detectable as a linear transcript (*3*, *9*, *10*). Human CDR1as, which is mainly located in the cytoplasm, has over 70 binding sites for the microRNA miR-7 (*3*, *9*), which is involved in regulation of a number of genes in the brain (*11*–*13*). Binding of miR-7 to CDR1as has been shown in cell lines and, consequently, CDR1as has been proposed to function as a sponge for miR-7 by reducing the number of freely available miR-7 molecules (*3*, *9*). The miR-7 binding sites are only partially complementary to miR-7, ensuring that Cdr1as is not sliced by Ago2 bound to miR-7:Cdr1as complexes. Cdr1as also has a binding site for miR-671 (*10*). This binding site, in contrast to the miR-7, has almost full complementarity to miR-671 and therefore may be used by miR-671 to mediate slicing of Cdr1as (*10*), potentially to release its miR-7 cargo. However, the normal in vivo function of Cdr1as is unknown.

Results

Cdr1as binding by miR-7 and miR-671 in the mammalian brain

To identify miRNAs that bind Cdr1as in the mammalian

brain, we utilized the recent finding that after RNA:protein purification of the miRNA effector AGO via cross-linking and immunoprecipitation ("CLIP" assays), the 3′ end of miRNAs can be ligated to the 5′ end of their RNA target sites. After sequencing, these so-called "chimeras" allow unambiguous in vivo detection of miRNA target sites as well as, simultaneously, the identification of the individual miRNAs bound to them (*14*). Using our computational pipeline for chimera detection (*14*), we identified and mapped tens of thousands of chimeras in recently published AGO CLIP data for mouse and human postmortem brains (*15*, *16*). When ranking these transcripts by the number of miR-7 chimeras mapping to an individual transcript, the top scoring target of all transcripts in both human and mouse brains was Cdr1as (Fig. 1A and table S1). Only one other miRNA was highly bound to Cdr1as (Fig. 1A), miR-671. However, in contrast to miR-7 for which we detect many distinct Cdr1as binding sites, we detected only one main binding site for miR-671 (Fig. 1A and table S1). The architecture of the miR-7 and miR-671 binding sites is also very different. While miR-7 sites feature complementarity only to the 5′ end ("seed" region, which is essential for the binding of the miRNA to mRNA) of miR-7, the miR-671 site is almost perfectly complementary to the entire mature miR-671 sequence (fig. S1). Therefore, miR-671 can mediate slicing of Cdr1as while miR-7 cannot. Strikingly, these binding site architectures are perfectly conserved during mammalian evolution (fig. S1), indicating that they are linked to the function of Cdr1as.

In our chimera analysis, the lncRNA Cyrano (1700020I14Rik) was identified as a second top-ranked RNA interacting with miR-7 in the mouse brain (table S1). Cyrano harbors a single, nearly perfect complementary and highly conserved binding site for miR-7 (*17*). These observations imply that next to Cdr1as, Cyrano may play an important role in the regulation of miR-7 in the central nervous system.

Neural expression pattern of Cdr1as

To determine Cdr1as expression patterns in the mouse brain, we performed RNA fluorescence in situ hybridization (FISH) in adult brain sections (Fig. 1B and figs. S2 to S4). Co-staining with neural markers revealed that Cdr1as was highly expressed in neurons but not expressed in glial cells such as oligodendrocytes and astrocytes (Fig. 1B and fig. S3D). Further, an overlap with excitatory and inhibitory neuronal markers showed that Cdr1as was predominantly expressed in excitatory and less in inhibitory neurons (Fig. 1, B and C, and figs. S2 to S4). In the cortex, hippocampus, midbrain and hindbrain, the majority of neurons expressing Cdr1as were vGluT1 and vGlutT2-positive (figs. S2, B to E; S3, A to C; and S4, B and D). In the cerebellum, Cdr1as expression was observed exclusively in the granular layer featuring high content of excitatory neurons and did not overlap with GABAergic neurons present in the molecular layer and Purkinje cells (fig. S4D). Single molecule RNA fluorescence in situ hybridization (smRNA FISH) in primary cortical neurons revealed Cdr1as expression in both soma and neurites (Fig. 1C, left), indicating a possible functional role of Cdr1as in different subcellular localizations.

Cdr1as loss-of-function mutant mice

As Cdr1as is so efficiently circularized in human and mouse cells that it cannot be detected as a linear transcript (*3*, *9*, *10*), the most straightforward strategy to create a loss-of-function (LoF) mouse model for this circRNA is to remove the *Cdr1as* locus by CRISPR/Cas9. However, this strategy could also affect transcription on the other strand and, therefore, complicate the interpretation. To evaluate expression from the other strand, we created and sequenced 24 stranded RNA libraries (i.e., retaining the strand-of-origin information in the RNA-seq library) from 4 mouse brain regions, performed in situ hybridization (ISH) with a probe complementary to putative sense transcript (Cdr1 mRNA), and analyzed published RNA-seq, CAGE and chromatin modification data (fig. S5). We failed to detect in mouse brains, specific mouse brain regions or any other mouse or human tissue analyzed, any evidence for transcription of the strand opposite to *Cdr1as*. We therefore proceeded and successfully removed the *Cdr1as* locus (Fig. 1D) from the mouse genome, as shown by genotyping (fig S6, A and B), in situ hybridization (Fig. 1D and fig. S6C), Northern blot analysis (fig. S6D) and qRT-PCRs (fig. S7A). *Cdr1as* knockout (KO) mice were viable, fertile and displayed no gross abnormality in adult brain anatomy (fig. S6E).

Because *Cdr1as* is X-linked, prior to analysis of knockout animals we sought to investigate Cdr1as expression in wild type (WT) male and female as well as heterozygous female ($Cdr1as^{+/-}$) brains. qRT-PCR assays showed that Cdr1as expression in male and female wild type mice was about equal, whereas in heterozygous female mice Cdr1as levels were reduced by approximately 50% relative to the wild type (fig. S7B). As there were no significant differences in Cdr1as expression levels between WT males and females, we used hemizygous male mice ($Cdr1as^{-/Y}$) for further molecular analysis.

miR-7 and miR-671 are post-transcriptionally deregulated in Cdr1as KO brain

We sequenced miRNAs in four major brain regions (cerebellum, cortex, hippocampus, and olfactory bulb) where Cdr1as is highly expressed (*7*). Northern blot analysis was also used to detect miR-7 in assayed tissues (fig. S8). When comparing expression levels from our sequencing data in WT and KO animals, miR-7 was consistently and markedly downregulat-

ed (Fig. 2, statistics in table S2). More precisely, both miR-7a-5p and miR-7b-5p, which have the same seed but slightly different mature sequences and are produced from three different miR-7 loci in the genome, were downregulated to comparable levels in all cases. This downregulation was highly specific. From hundreds of identified miRNAs, except miR-7a-5p and miR-7b-5p, only eight other miRNAs were significantly downregulated, and this occurred only in the cortex (Fig. 2B). All these miRNAs belong to two families and are derived from three primary transcripts (miR-200c/141, miR-200a/200b/429, and miR-182/183/96). We confirmed miR-7 downregulation in all four brain regions by Northern blot (Fig. 3A and fig. S9) as well as in situ hybridization (Fig. 3, B and C) and qRT-PCR assays (fig. S7C). Moreover, miR-7 downregulation was post-transcriptional. This is supported by the sequencing data showing that all three miR-7 passenger strands (miR-7a-1-3p, miR-7a-2-3p, miR-7b-3p), which are processed from the respective three distinct miR-7 precursors, are not significantly deregulated (Fig. 2). This observation was validated by Northern blot (fig. S9A) and an independent qRT-PCR assay for pre-miR-7a-1 (fig. S7D). pre-miR-7a-2 and pre-miR-7b were below reliable detection levels in qRT-PCR analysis. The downregulated expression of miRNAs from miR-200 and miR-183 families in cortex was probably due to a transcriptional effect as the corresponding passenger strands are also downregulated (Fig. 2B). Contrary to miR-7, miR-671-5p expression in KO animals was upregulated in the cerebellum, cortex, and olfactory bulb (Fig. 2, A, B, and D). Similarly to miR-7, this deregulation in KO mice was highly specific – aside from miR-671, no other miRNA was consistently upregulated. Also similar to miR-7, miR-671-5p was upregulated post-transcriptionally, as can be seen by unperturbed passenger strand expression (Fig. 2, A, B, and D). Northern blot analysis failed to detect mature miR-671-5p both in KO and WT RNA extracts, although miR-671-3p was detectable and remained unaltered (fig. S9A). Two reasons may explain why miR-671-5p and its precursor are difficult to detect: (i) mature miR-671 is lowly expressed and unstable as shown in metabolic labeling experiments (*18*), and (ii) the precursor is processed from coding sequence of the well-expressed *Chpf2* transcript.

We analyzed Cdr1as, miR-7, and miR-671 levels in non-brain tissues: lung, skeletal muscle, spleen, heart, spinal cord (fig. S7, A, C, and E). In the spleen, where Cdr1as was undetectable but miR-7a was well-expressed, and other tissues exhibiting very low expression of Cdr1as, the level of miR-7a was not changed by *Cdr1as* removal. The only non-brain tissue with substantially changed miR-7 expression was spinal cord. This was also the only non-brain tissue for which we detected reasonable expression of Cdr1as, in line with Cdr1as expression in neurons and neuronal projections. Taken together, these data show that loss of Cdr1as does not affect miR-7 and miR-671 in tissues outside the brain which normally exhibit very low levels or Cdr1as RNA, whereas downregulation of miR-7 in neural tissues of KO animals is dependent on Cdr1as loss. We conclude that there is a highly specific, post-transcriptional deregulation of miR-7 and miR-671 in the brains of *Cdr1as* KO animals. These are the two miRNAs we identified by in vivo chimera analysis to directly interact with Cdr1as.

Upregulation of immediate early genes, including miR-7 targets, in Cdr1as KO brain

To assess the functional consequences of Cdr1as removal, we measured changes in mRNA expression by sequencing mRNAs in the same brain regions in which we had observed miR-7/miR-671 deregulation - cerebellum, cortex, hippocampus, and olfactory bulb (Fig. 4, A to D, and table S3). Conserved miR-7 targets (*19*) were significantly upregulated in cortex, cerebellum and olfactory bulb (Mann-Whitney U test, p-value < 10^{-4}, 10^{-3}, and 10^{-7}, respectively) (fig. S10), including several validated miR-7 targets such as *Fos,* a well-known direct miR-7 target with three conserved binding sites in its 3′ UTR (*20*), *Nr4a3* (*21*), *Irs2* (*22*) or *Klf4* (*23*) (Fig. 4, A to D; fig. S11; and statistics in tables S3 and S4). The lncRNA Cyrano, which interacts with miR-7 in the brain, as supported by Cyrano:miR-7 chimeras (table S1), was highly expressed and stable in all analyzed brain regions of *Cdr1as* knockout animals. Furthermore, inspection of the genes upregulated in each of the four brain regions revealed an obvious and highly significant overrepresentation (hypergeometric test p-value < 10^{-33}) of immediate early genes (IEGs), which are part of the first wave of response to different stimuli and markers of neuronal activity, such as *Fos*, *Arc*, *Egr1*, *Egr2*, *Nr4a3*, and others (Fig. 4, A to D; fig. S11; and tables S3 and S4). We validated the sequencing data by qRT-PCRs (fig. S12) and Nanostring (fig. S13A and table S5) using the cortex and hippocampus from the same and independent animals. We confirmed an increased expression of IEGs at the protein level for all tested candidates. Elevated levels of c-Fos, Egr1, and Arc were detected by Western blots (Fig. 4E), and by further immunohistochemical validation of c-Fos and Egr1 proteins in brain sections (Fig. 4F and figs. S14 to S16). c-Fos immunostaining performed in four cortical regions was quantified, revealing consistent increase in both number of neurons expressing c-Fos, and c-Fos signal intensity in KO (fig. S15). These data are important for two reasons. First, miR-7 is a known repressor of the cell cycle and IEGs such as *Fos*, suggesting a direct link between Cdr1as removal and upregulation of IEGs. Second, upregulation of IEGs is strongly linked to increased activity of neurons (*24–26*). Therefore, we conclude that the reduction of miR-7 followed by enhanced expres-

sion of IEGs implies higher neuronal activity in *Cdr1as* KO brains, and hypothesized that this effect has further functional consequences at the phenotypic level.

The expression levels of IEGs in non-brain tissues of KO animals remained unaltered (fig. S13, B to E), suggesting that the observed effect was brain-specific and consistent with the expression pattern of Cdr1as. We also observed that in addition to IEGs, there were several differentially expressed circadian clock genes in *Cdr1as* KO brains. *Per1* and *Sik1* were consistently upregulated, and *Dbp* was consistently downregulated (Fig. 4, A to D). This expression pattern in the forebrain has previously been associated with sleep deprivation and extended wakefulness in mice (*27*, *28*).

Dysfunction of excitatory synaptic transmission in Cdr1as KO mice

As Cdr1as is predominantly expressed in excitatory neurons (Fig. 1, B and C, and figs. S2 to S4) we wanted to elucidate the physiological consequences of removal of Cdr1as at the synaptic level. Therefore, we utilized single hippocampal neurons and studied excitatory postsynaptic currents (EPSCs). We found that spontaneous vesicle release was strongly upregulated in the KO neurons with more than a doubling of miniature excitatory postsynaptic currents (mEPSC) frequency (Fig. 5A) but not amplitude (fig. S17A). By analyzing calcium-evoked synaptic responses, we noted that the EPSC amplitude of Cdr1as KO neurons was not significantly different from WT neurons (Fig. 5B, left). The observed effect of higher spontaneous release was not dependent on synapse formation or vesicle priming activity, as the size of the readily releasable vesicle pool was not significantly altered (fig. S17B). Although the computed vesicular release probability was not significantly altered (fig. S17B), responses to two consecutive stimuli (Fig. 5B, right), and to a train of action potentials at 10 Hz, were differentially modulated in the KO vs. WT (fig. S17C). This suggests an altered vesicle replenishment dynamics during ongoing synaptic release activity and stronger depression in the synaptic response in the KO neurons. Taken together, these electrophysiological recordings indicate that Cdr1as deficiency leads to a dysfunction of excitatory synaptic transmission. Possible mechanisms that could explain this change include: changes in expression of synaptic proteins (*29*), malformation of synaptic specialization, or alteration in synaptic calcium homeostasis (*30*).

Neuropsychiatric-like alteration in the behavior of Cdr1as KO mice

To further evaluate the biological implications of miRNA and IEGs deregulation in *Cdr1as* KO brains, we performed behavioral assays with WT and *Cdr1as* KO animals (Fig. 5C, fig. S18, and table S6). *Cdr1as* knockout mice showed normal social behavior, unaffected anxiety levels, unperturbed locomotor activity in open field test, and no significant deficits in recognition memory or exploratory behavior (fig. S18, B to H). Contrary to these assays, prepulse inhibition (PPI) of the startle response test revealed a significant and strong (between 30-50%) difference between WT and *Cdr1as* KO males and females at all three prepulse intensities (Fig. 5C). PPI is used to detect defects in the normal suppression of the startle response that occurs when a startle-eliciting stimulus is preceded by a low-intensity prestimulus (the prepulse). It is a measure of sensorimotor gating which is impaired in schizophrenia and some other psychiatric diseases in humans and used in animal models of endophenotypes related to neuropsychiatric disorders (*31–34*). The impairment was evident and specific for the inhibition of the startle response. The baseline response to the pulse only (120 dB) was similar across genotypes and groups (fig. S18A). Therefore, the PPI deficiency is not due to differences in the response to an acoustic stimulus or due to hearing impairments.

Taken together, our data provide evidence that *Cdr1as* KO animals exhibit a behavioral phenotype associated with neuropsychiatric disorders reflected in a strong sensorimotor gating deficit. Our findings support the general observation that upregulation of IEGs such as *Fos*, *Egr1*, *Egr4* is linked to reduced PPI (*35*).

Discussion

Here, we used CRISPR/Cas9 to remove the locus encoding Cdr1as, a circRNA highly expressed in neurons and predominantly localized to the cytoplasm. In all tested in vivo mammalian tissues and cell lines, Cdr1as was detected only as a circular RNA (*3*, *9*, *10*). We failed, by different assays, to detect any transcription on the strand antisense to *Cdr1as*, making it unlikely that removal of the *Cdr1as* locus has consequences beyond removing the circular RNA. We cannot rule out CRISPR/Cas9 off-target effects, but we believe that these (if existent) are unlikely to contribute to the molecular and behavioral phenotype that we observe in the KO animals. This is because (i) we show that precisely the two miRNAs (miR-7, miR-671) that we find to specifically interact with Cdr1as in the brain are deregulated in the KO animals, (ii) immediate early genes (IEGs), including direct targets of miR-7, are upregulated in the mutant brains but not in other tissues where Cdr1as is very lowly or not expressed, (iii) IEGs are already known to be linked to the observed neuropsychiatric symptom - impaired prepulse inhibition (PPI) (*35*), and (iv) Cdr1as is exclusively expressed in neurons but not glial cells, suggesting that Cdr1as interactions with miRNAs are functional in neurons and thus in line with the observed deficit in PPI and dysfunction in synaptic transmission.

How can we explain the specific and opposite deregulation of miR-7 and miR-671 upon loss of Cdr1as? The reason may lie in the very different and highly conserved architecture of the binding sites of miR-7 and miR-671 on Cdr1as. None of the >70 miR-7 binding sites has significant complementarity beyond the seed region, indicating that miR-7 stably binds but cannot slice Cdr1as. In contrast, miR-671 has one main binding site with almost perfect complementarity, which should lead to slicing of Cdr1as (*10*) and may cause tailing and trimming (i.e., removal) of miR-671 (*36*, *37*). Thus, upon depletion of Cdr1as, we expect upregulation of miR-671 and downregulation of miR-7, which is no longer stabilized by Cdr1as.

Is miR-7 turnover upon KO of Cdr1as a passive decay process or is it regulated? We speculate that miR-7 decay is promoted and regulated by the Cyrano lncRNA (*17*). This is because (i) we found Cyrano to be the second-highest miR-7 interactor in chimeric data (table S1), (ii) Cyrano was well expressed in all tissues in which we detected Cdr1as expression (Fig. 4, A to D), (iii) the miR-7 binding site on Cyrano is unusual in that it has extremely well conserved architecture which, similar to the miR-671 binding site on Cdr1as, could promote miR-7 removal by tailing and trimming (*17*, *36*, *37*).

When comparing mRNA expression between WT and KO animals, we found an enrichment for upregulated IEGs, some of which, like *Fos* and *Nr4a3*, are known miR-7 targets. In fact, upregulation of predicted miR-7 targets was statistically significant, consistent with the observed reduction of miR-7. The known miR-7 targets *Klf4*, *Nr4a3* and *Irs2,* which were increased in KO postnatal cortex, were also upregulated in a miR-7 knockdown study performed in the embryonic cortex (*13*). However, miR-7 targets did not explain the majority of upregulation, indicating that we observed a mixture of direct and indirect effects. We also noted different overall responses of miR-7 targets in the mouse brain upon constitutive *Cdr1as* knockout compared to knockdown experiments in HEK293 cells, in which targets of miR-7 were repressed (*3*). We argue that there are different scenarios for what may happen to miR-7 bound to Cdr1as if Cdr1as is removed from a cellular system conditionally vs. constitutively. A scenario in which miR-7:RISC complexes could be released and subsequently can downregulate miR-7 targets may be more plausible when Cdr1as is conditionally knocked down. In a situation in which Cdr1as is constitutively knocked out, miR-7 molecules not stabilized by the circle may have a higher probability to be turned over. Thus, miR-7 targets can be up-regulated. Additionally, the widespread distribution of Cdr1as in neuronal processes argues for a functional role of Cdr1as in transport of miR-7:AGO complexes and provides another layer of complexity to regulation of miR-7 targets, which could be regulated differentially in various subcellular localizations. We note that miR-671 therefore may provide an "unlocking" mechanism which serves to slice Cdr1as upon specific conditions within the cell to release the cargo (sponged miR-7:AGO complexes). It will be interesting to test these hypotheses, but the lack of suitable in vitro systems, technical difficulties in performing efficient, conditional overexpression or knockdown of Cdr1as, and the complex phenotypes observed will likely require the generation of many transgenic cell and mouse lines.

In any case, activation of IEGs has been linked to increased neuronal activity, which can be induced by both cell-extrinsic and cell-intrinsic signals (*38*, *39*) and has further functional consequences *e.g.* in synaptic plasticity and memory formation (*40*).

In behavioral tests, *Cdr1as* KO animals displayed significant and strong PPI impairment which indicates a neuropsychiatric phenotype. Deficits in PPI are reflected as the inability to effectively attenuate the intrinsic startle response to redundant stimuli. PPI deficit correlates clinically with symptoms such as thought disorder and distractibility in schizophrenia, therefore PPI emerged as a promising endophenotype in human and rodent models of the disease (*31*, *33*, *41*). Reduced PPI is also a hallmark of other neuropsychiatric disorders including obsessive compulsive disorder, bipolar disorder, Tourette syndrome, post-traumatic stress disorder, Huntington disease and Asperger syndrome (*34*, *42*). PPI is a complex phenotype that involves diverse neural systems encompassing the brainstem, peduncolopontine, hippocampus, amygdala and prefrontal cortical regions as well as different neurochemical substrates including dopamine, glutamate and GABA (*43*). According to our analysis Cdr1as is expressed in the majority of excitatory neurons. After removing the *Cdr1as* locus, we observed a disrupted excitatory neurotransmission reflected as an increased spontaneous vesicle release and stronger depression in synaptic response upon enhanced neuronal activity in KO neurons. In this context it is interesting to note that miR-7 has been described as negative regulator of vesicle release in pancreatic β cells (*44*). Our findings suggest that loss of Cdr1as destabilizes mature miR-7 in neurons, which results in de-repression of IEGs and leads to an altered neuronal activity, which may cause the sensorimotor deficits and the neuropsychiatric phenotype. Given the broad expression of Cdr1as in the brain and the diversity of the neural systems recruited in PPI, clearly, this hypothesis needs thorough testing.

In this study we focused on behavior and synaptic functions. However, we noticed that genes specific for circadian clock regulation are consistently deregulated in KO brains. Moreover, miR-7, miR-671, the miR-200 family and IEGs are associated with cancer, which will be important to follow up in cancer models in the future.

Methods summary

Cdr1as knockout (KO) animals were generated using CRISPR/Cas9 via microinjection of one-cell embryos with Cas9 mRNA and two sgRNAs designed to bind upstream of *Cdr1as* splice sites. The *Cdr1as* KO strain was generated and maintained on the pure C57BL/6N background. Molecular and electrophysiological analyses were performed using knockouts and littermate wild-type control animals. Behavioral studies were performed using *Cdr1as* KO animals, littermate or age-matched wild-type control animals. The experimental procedures were approved by the Landesamt für Gesundheit and Soziales (Berlin, Germany).

In situ hybridization and immunostainings were performed on fresh frozen brain sections using locked nucleic acid probes, RNAs obtained by in vitro transcription on PCR products or commercially available antibodies. Whole-cell voltage-clamp recordings were obtained from *Cdr1as* KO and WT hippocampal autaptic neurons at day 14-17 in vitro. cDNA libraries for RNA-Seq were generated according to the Illumina TruSeq protocols and sequenced on an Illumina NextSeq 500 System. Differential gene/miRNA expression analyses were performed using the DESeq2 package. RNA:miRNA chimeric reads were analyzed using previously published AGO HITS-CLIP data (*15*, *16*) and an in-house pipeline based on (*14*). The details of experimental procedures, reagents and computational analyses, including supporting references, are given in the materials and methods section of the supplementary materials.

REFERENCES AND NOTES

1. J. Salzman, C. Gawad, P. L. Wang, N. Lacayo, P. O. Brown, Circular RNAs are the predominant transcript isoform from hundreds of human genes in diverse cell types. *PLOS ONE* **7**, e30733 (2012). doi:10.1371/journal.pone.0030733 Medline
2. W. R. Jeck, J. A. Sorrentino, K. Wang, M. K. Slevin, C. E. Burd, J. Liu, W. F. Marzluff, N. E. Sharpless, Circular RNAs are abundant, conserved, and associated with ALU repeats. *RNA* **19**, 141–157 (2013). doi:10.1261/rna.035667.112 Medline
3. S. Memczak, M. Jens, A. Elefsinioti, F. Torti, J. Krueger, A. Rybak, L. Maier, S. D. Mackowiak, L. H. Gregersen, M. Munschauer, A. Loewer, U. Ziebold, M. Landthaler, C. Kocks, F. le Noble, N. Rajewsky, Circular RNAs are a large class of animal RNAs with regulatory potency. *Nature* **495**, 333–338 (2013). doi:10.1038/nature11928 Medline
4. R. Ashwal-Fluss, M. Meyer, N. R. Pamudurti, A. Ivanov, O. Bartok, M. Hanan, N. Evantal, S. Memczak, N. Rajewsky, S. Kadener, circRNA biogenesis competes with pre-mRNA splicing. *Mol. Cell* **56**, 55–66 (2014). doi:10.1016/j.molcel.2014.08.019 Medline
5. X. O. Zhang, H.-B. Wang, Y. Zhang, X. Lu, L.-L. Chen, L. Yang, Complementary sequence-mediated exon circularization. *Cell* **159**, 134–147 (2014). doi:10.1016/j.cell.2014.09.001 Medline
6. S. Starke, I. Jost, O. Rossbach, T. Schneider, S. Schreiner, L.-H. Hung, A. Bindereif, Exon circularization requires canonical splice signals. *Cell Rep.* **10**, 103–111 (2015). doi:10.1016/j.celrep.2014.12.002 Medline
7. A. Rybak-Wolf, C. Stottmeister, P. Glažar, M. Jens, N. Pino, S. Giusti, M. Hanan, M. Behm, O. Bartok, R. Ashwal-Fluss, M. Herzog, L. Schreyer, P. Papavasileiou, A. Ivanov, M. Öhman, D. Refojo, S. Kadener, N. Rajewsky, Circular RNAs in the mammalian brain are highly abundant, conserved, and dynamically expressed. *Mol. Cell* **58**, 870–885 (2015). doi:10.1016/j.molcel.2015.03.027 Medline
8. X. You, I. Vlatkovic, A. Babic, T. Will, I. Epstein, G. Tushev, G. Akbalik, M. Wang, C. Glock, C. Quedenau, X. Wang, J. Hou, H. Liu, W. Sun, S. Sambandan, T. Chen, E. M. Schuman, W. Chen, Neural circular RNAs are derived from synaptic genes and regulated by development and plasticity. *Nat. Neurosci.* **18**, 603–610 (2015). doi:10.1038/nn.3975 Medline
9. T. B. Hansen, T. I. Jensen, B. H. Clausen, J. B. Bramsen, B. Finsen, C. K. Damgaard, J. Kjems, Natural RNA circles function as efficient microRNA sponges. *Nature* **495**, 384–388 (2013). doi:10.1038/nature11993 Medline
10. T. B. Hansen, E. D. Wiklund, J. B. Bramsen, S. B. Villadsen, A. L. Statham, S. J. Clark, J. Kjems, miRNA-dependent gene silencing involving Ago2-mediated cleavage of a circular antisense RNA. *EMBO J.* **30**, 4414–4422 (2011). doi:10.1038/emboj.2011.359 Medline
11. E. Junn, K.-W. Lee, B. S. Jeong, T. W. Chan, J.-Y. Im, M. M. Mouradian, Repression of α-synuclein expression and toxicity by microRNA-7. *Proc. Natl. Acad. Sci. U.S.A.* **106**, 13052–13057 (2009). doi:10.1073/pnas.0906277106 Medline
12. A. de Chevigny, N. Coré, P. Follert, M. Gaudin, P. Barbry, C. Béclin, H. Cremer, miR-7a regulation of Pax6 controls spatial origin of forebrain dopaminergic neurons. *Nat. Neurosci.* **15**, 1120–1126 (2012). doi:10.1038/nn.3142 Medline
13. A. Pollock, S. Bian, C. Zhang, Z. Chen, T. Sun, Growth of the developing cerebral cortex is controlled by microRNA-7 through the p53 pathway. *Cell Rep.* **7**, 1184–1196 (2014). doi:10.1016/j.celrep.2014.04.003 Medline
14. S. Grosswendt, A. Filipchyk, M. Manzano, F. Klironomos, M. Schilling, M. Herzog, E. Gottwein, N. Rajewsky, Unambiguous identification of miRNA:target site interactions by different types of ligation reactions. *Mol. Cell* **54**, 1042–1054 (2014). doi:10.1016/j.molcel.2014.03.049 Medline
15. R. L. Boudreau, P. Jiang, B. L. Gilmore, R. M. Spengler, R. Tirabassi, J. A. Nelson, C. A. Ross, Y. Xing, B. L. Davidson, Transcriptome-wide discovery of microRNA binding sites in human brain. *Neuron* **81**, 294–305 (2014). doi:10.1016/j.neuron.2013.10.062 Medline
16. M. J. Moore, T. K. H. Scheel, J. M. Luna, C. Y. Park, J. J. Fak, E. Nishiuchi, C. M. Rice, R. B. Darnell, miRNA-target chimeras reveal miRNA 3′-end pairing as a major determinant of Argonaute target specificity. *Nat. Commun.* **6**, 8864 (2015). doi:10.1038/ncomms9864 Medline
17. I. Ulitsky, A. Shkumatava, C. H. Jan, H. Sive, D. P. Bartel, Conserved function of lincRNAs in vertebrate embryonic development despite rapid sequence evolution. *Cell* **147**, 1537–1550 (2011). doi:10.1016/j.cell.2011.11.055 Medline
18. E. E. Duffy, M. Rutenberg-Schoenberg, C. D. Stark, R. R. Kitchen, M. B. Gerstein, M. D. Simon, Tracking distinct RNA populations using efficient and reversible covalent chemistry. *Mol. Cell* **59**, 858–866 (2015). doi:10.1016/j.molcel.2015.07.023 Medline
19. V. Agarwal, G. W. Bell, J. W. Nam, D. P. Bartel, Predicting effective microRNA target sites in mammalian mRNAs. *eLife* **4**, e05005 (2015). doi:10.7554/eLife.05005 Medline
20. X. D. Zhao, Y.-Y. Lu, H. Guo, H.-H. Xie, L.-J. He, G.-F. Shen, J.-F. Zhou, T. Li, S.-J. Hu, L. Zhou, Y.-N. Han, S.-L. Liang, X. Wang, K.-C. Wu, Y.-Q. Shi, Y.-Z. Nie, D.-M. Fan, MicroRNA-7/NF-κB signaling regulatory feedback circuit regulates gastric carcinogenesis. *J. Cell Biol.* **210**, 613–627 (2015). doi:10.1083/jcb.201501073 Medline
21. L. Stevanato, J. D. Sinden, The effects of microRNAs on human neural stem cell differentiation in two- and three-dimensional cultures. *Stem Cell Res. Ther.* **5**, 49 (2014). doi:10.1186/scrt437 Medline
22. K. M. Giles, R. A. Brown, M. R. Epis, F. C. Kalinowski, P. J. Leedman, miRNA-7-5p inhibits melanoma cell migration and invasion. *Biochem. Biophys. Res. Commun.* **430**, 706–710 (2013). doi:10.1016/j.bbrc.2012.11.086 Medline
23. H. Okuda, F. Xing, P. R. Pandey, S. Sharma, M. Watabe, S. K. Pai, Y.-Y. Mo, M. Iiizumi-Gairani, S. Hirota, Y. Liu, K. Wu, R. Pochampally, K. Watabe, miR-7 suppresses brain metastasis of breast cancer stem-like cells by modulating KLF4. *Cancer Res.* **73**, 1434–1444 (2013). doi:10.1158/0008-5472.CAN-12-2037 Medline
24. W. C. Abraham, S. E. Mason, J. Demmer, J. M. Williams, C. L. Richardson, W. P. Tate, P. A. Lawlor, M. Dragunow, Correlations between immediate early gene induction and the persistence of long-term potentiation. *Neuroscience* **56**, 717–727 (1993). doi:10.1016/0306-4522(93)90369-Q Medline
25. J. I. Morgan, D. R. Cohen, J. L. Hempstead, T. Curran, Mapping patterns of c-fos expression in the central nervous system after seizure. *Science* **237**, 192–197 (1987). doi:10.1126/science.3037702 Medline
26. J. F. Guzowski, B. L. McNaughton, C. A. Barnes, P. F. Worley, Environment-

specific expression of the immediate-early gene Arc in hippocampal neuronal ensembles. *Nat. Neurosci.* **2**, 1120–1124 (1999). doi:10.1038/16046 Medline
27. J. P. Wisor, B. F. O'Hara, A. Terao, C. P. Selby, T. S. Kilduff, A. Sancar, D. M. Edgar, P. Franken, A role for cryptochromes in sleep regulation. *BMC Neurosci.* **3**, 20 (2002). doi:10.1186/1471-2202-3-20 Medline
28. P. Franken, R. Thomason, H. C. Heller, B. F. O'Hara, A non-circadian role for clock-genes in sleep homeostasis: A strain comparison. *BMC Neurosci.* **8**, 87 (2007). doi:10.1186/1471-2202-8-87 Medline
29. J. Rizo, C. Rosenmund, Synaptic vesicle fusion. *Nat. Struct. Mol. Biol.* **15**, 665–674 (2008). doi:10.1038/nsmb.1450 Medline
30. E. T. Kavalali, The mechanisms and functions of spontaneous neurotransmitter release. *Nat. Rev. Neurosci.* **16**, 5–16 (2015). doi:10.1038/nrn3875 Medline
31. J. Pratt, C. Winchester, N. Dawson, B. Morris, Advancing schizophrenia drug discovery: Optimizing rodent models to bridge the translational gap. *Nat. Rev. Drug Discov.* **11**, 560–579 (2012). doi:10.1038/nrd3649 Medline
32. S. A. Wolf, A. Melnik, G. Kempermann, Physical exercise increases adult neurogenesis and telomerase activity, and improves behavioral deficits in a mouse model of schizophrenia. *Brain Behav. Immun.* **25**, 971–980 (2011). doi:10.1016/j.bbi.2010.10.014 Medline
33. M. A. Geyer, K. L. McIlwain, R. Paylor, Mouse genetic models for prepulse inhibition: An early review. *Mol. Psychiatry* **7**, 1039–1053 (2002). doi:10.1038/sj.mp.4001159 Medline
34. D. L. Braff, M. A. Geyer, N. R. Swerdlow, Human studies of prepulse inhibition of startle: Normal subjects, patient groups, and pharmacological studies. *Psychopharmacology* **156**, 234–258 (2001). doi:10.1007/s002130100810 Medline
35. A. J. Grottick, D. Bagnol, S. Phillips, J. McDonald, D. P. Behan, D. T. Chalmers, Y. Hakak, Neurotransmission- and cellular stress-related gene expression associated with prepulse inhibition in mice. *Brain Res. Mol. Brain Res.* **139**, 153–162 (2005). doi:10.1016/j.molbrainres.2005.05.020 Medline
36. S. L. Ameres, M. D. Horwich, J.-H. Hung, J. Xu, M. Ghildiyal, Z. Weng, P. D. Zamore, Target RNA-directed trimming and tailing of small silencing RNAs. *Science* **328**, 1534–1539 (2010). doi:10.1126/science.1187058 Medline
37. M. de la Mata, D. Gaidatzis, M. Vitanescu, M. B. Stadler, C. Wentzel, P. Scheiffele, W. Filipowicz, H. Großhans, Potent degradation of neuronal miRNAs induced by highly complementary targets. *EMBO Rep.* **16**, 500–511 (2015). doi:10.15252/embr.201540078 Medline
38. H. Okuno, Regulation and function of immediate-early genes in the brain: Beyond neuronal activity markers. *Neurosci. Res.* **69**, 175–186 (2011). doi:10.1016/j.neures.2010.12.007 Medline
39. S. Bahrami, F. Drabløs, Gene regulation in the immediate-early response process. *Adv. Biol. Regul.* **62**, 37–49 (2016). doi:10.1016/j.jbior.2016.05.001 Medline
40. K. Minatohara, M. Akiyoshi, H. Okuno, Role of immediate-early genes in synaptic plasticity and neuronal ensembles underlying the memory trace. *Front. Mol. Neurosci.* **8**, 78 (2016). Medline
41. D. Braff, C. Stone, E. Callaway, M. Geyer, I. Glick, L. Bali, Prestimulus effects on human startle reflex in normals and schizophrenics. *Psychophysiology* **15**, 339–343 (1978). doi:10.1111/j.1469-8986.1978.tb01390.x Medline
42. G. M. McAlonan, E. Daly, V. Kumari, H. D. Critchley, T. van Amelsvoort, J. Suckling, A. Simmons, T. Sigmundsson, K. Greenwood, A. Russell, N. Schmitz, F. Happe, P. Howlin, D. G. Murphy, Brain anatomy and sensorimotor gating in Asperger's syndrome. *Brain* **125**, 1594–1606 (2002). doi:10.1093/brain/awf150 Medline
43. N. R. Swerdlow, M. A. Geyer, D. L. Braff, Neural circuit regulation of prepulse inhibition of startle in the rat: Current knowledge and future challenges. *Psychopharmacology* **156**, 194–215 (2001). doi:10.1007/s002130100799 Medline
44. M. Latreille, J. Hausser, I. Stützer, Q. Zhang, B. Hastoy, S. Gargani, J. Kerr-Conte, F. Pattou, M. Zavolan, J. L. S. Esguerra, L. Eliasson, T. Rülicke, P. Rorsman, M. Stoffel, MicroRNA-7a regulates pancreatic β cell function. *J. Clin. Invest.* **124**, 2722–2735 (2014). doi:10.1172/JCI73066 Medline
45. F. A. Ran, P. D. Hsu, J. Wright, V. Agarwala, D. A. Scott, F. Zhang, Genome engineering using the CRISPR-Cas9 system. *Nat. Protoc.* **8**, 2281–2308 (2013). doi:10.1038/nprot.2013.143 Medline
46. L. Cong, F. A. Ran, D. Cox, S. Lin, R. Barretto, N. Habib, P. D. Hsu, X. Wu, W. Jiang, L. A. Marraffini, F. Zhang, Multiplex genome engineering using CRISPR/Cas systems. *Science* **339**, 819–823 (2013). doi:10.1126/science.1231143 Medline
47. C. Brandl, O. Ortiz, B. Röttig, B. Wefers, W. Wurst, R. Kühn, Creation of targeted genomic deletions using TALEN or CRISPR/Cas nuclease pairs in one-cell mouse embryos. *FEBS Open Bio* **5**, 26–35 (2014). doi:10.1016/j.fob.2014.11.009 Medline
48. L. M. Ittner, J. Götz, Pronuclear injection for the production of transgenic mice. *Nat. Protoc.* **2**, 1206–1215 (2007). doi:10.1038/nprot.2007.145 Medline
49. X. Adiconis, D. Borges-Rivera, R. Satija, D. S. DeLuca, M. A. Busby, A. M. Berlin, A. Sivachenko, D. A. Thompson, A. Wysoker, T. Fennell, A. Gnirke, N. Pochet, A. Regev, J. Z. Levin, Comparative analysis of RNA sequencing methods for degraded or low-input samples. *Nat. Methods* **10**, 623–629 (2013). doi:10.1038/nmeth.2483 Medline
50. A. Dobin, C. A. Davis, F. Schlesinger, J. Drenkow, C. Zaleski, S. Jha, P. Batut, M. Chaisson, T. R. Gingeras, STAR: Ultrafast universal RNA-seq aligner. *Bioinformatics* **29**, 15–21 (2013). doi:10.1093/bioinformatics/bts635 Medline
51. S. Anders, P. T. Pyl, W. Huber, HTSeq—a Python framework to work with high-throughput sequencing data. *Bioinformatics* **31**, 166–169 (2015). doi:10.1093/bioinformatics/btu638 Medline
52. B. L. Aken, S. Ayling, D. Barrell, L. Clarke, V. Curwen, S. Fairley, J. Fernandez Banet, K. Billis, C. García Girón, T. Hourlier, K. Howe, A. Kähäri, F. Kokocinski, F. J. Martin, D. N. Murphy, R. Nag, M. Ruffier, M. Schuster, Y. A. Tang, J.-H. Vogel, S. White, A. Zadissa, P. Flicek, S. M. J. Searle, The Ensembl gene annotation system. *Database* **2016**, baw093 (2016). doi:10.1093/database/baw093 Medline
53. M. I. Love, W. Huber, S. Anders, Moderated estimation of fold change and dispersion for RNA-seq data with DESeq2. *Genome Biol.* **15**, 550 (2014). doi:10.1186/s13059-014-0550-8 Medline
54. M. Dodt, J. T. Roehr, R. Ahmed, C. Dieterich, FLEXBAR—Flexible barcode and adapter processing for next-generation sequencing platforms. *Biology* **1**, 895–905 (2012). doi:10.3390/biology1030895 Medline
55. M. R. Friedländer, S. D. Mackowiak, N. Li, W. Chen, N. Rajewsky, miRDeep2 accurately identifies known and hundreds of novel microRNA genes in seven animal clades. *Nucleic Acids Res.* **40**, 37–52 (2012). doi:10.1093/nar/gkr688 Medline
56. A. Kozomara, S. Griffiths-Jones, miRBase: Annotating high confidence microRNAs using deep sequencing data. *Nucleic Acids Res.* **42**, D68–D73 (2014). doi:10.1093/nar/gkt1181 Medline
57. B. Langmead, S. L. Salzberg, Fast gapped-read alignment with Bowtie 2. *Nat. Methods* **9**, 357–359 (2012). doi:10.1038/nmeth.1923 Medline
58. J. W. Tullai, M. E. Schaffer, S. Mullenbrock, G. Sholder, S. Kasif, G. M. Cooper, Immediate-early and delayed primary response genes are distinct in function and genomic architecture. *J. Biol. Chem.* **282**, 23981–23995 (2007). doi:10.1074/jbc.M702044200 Medline
59. J. Krüger, M. Rehmsmeier, RNAhybrid: microRNA target prediction easy, fast and flexible. *Nucleic Acids Res.* **34**, W451–W454 (2006). doi:10.1093/nar/gkl243 Medline
60. R. C. Edgar, MUSCLE: Multiple sequence alignment with high accuracy and high throughput. *Nucleic Acids Res.* **32**, 1792–1797 (2004). doi:10.1093/nar/gkh340 Medline
61. L. R. Hernández-Miranda, A. Cariboni, C. Faux, C. Ruhrberg, J. H. Cho, J.-F. Cloutier, B. J. Eickholt, J. G. Parnavelas, W. D. Andrews, Robo1 regulates semaphorin signaling to guide the migration of cortical interneurons through the ventral forebrain. *J. Neurosci.* **31**, 6174–6187 (2011). doi:10.1523/JNEUROSCI.5464-10.2011 Medline
62. S. Kaech, G. Banker, Culturing hippocampal neurons. *Nat. Protoc.* **1**, 2406–2415 (2006). doi:10.1038/nprot.2006.356 Medline
63. C. Sampathkumar, Y.-J. Wu, M. Vadhvani, T. Trimbuch, B. Eickholt, C. Rosenmund, Loss of MeCP2 disrupts cell autonomous and autocrine BDNF signaling in mouse glutamatergic neurons. *eLife* **5**, e19374 (2016). doi:10.7554/eLife.19374 Medline
64. C. Rosenmund, C. F. Stevens, Definition of the readily releasable pool of vesicles at hippocampal synapses. *Neuron* **16**, 1197–1207 (1996). doi:10.1016/S0896-6273(00)80146-4 Medline

ACKNOWLEDGMENTS

We thank all members of the N. Rajewsky lab and the C. Birchmeier lab for helpful discussions and support. We thank M. Herzog for organizational help, M. Schilling for computational assistance, T. Müller for technical advice on the primary neuronal cultures and discussions. We thank G. Matz, A. Boltengagen, P. Stallerow, M. Terne, S. Buchert, R. Kabisch, A. Leschke, D. Schreiber and R. Dannenberg for their technical assistance. LRHM acknowledges the European Commission for funding under the scheme Marie Skłodowska-Curie (fellowship 302477). ARW acknowledges funding by BIH-grant CRG 2a TP7. SM was funded by the DFG grant RA 838/6-1. AF thanks the DFG Graduate School "Computational Systems Biology" CBS-GRK 1772 for a fellowship and the DZHK for funding. FK and PG acknowledge funding from DEEP (Deutsches Epigenom Programm). SAW is supported by a DFG grant WO 1418/3-1. CACJ is funded by the MDC graduate program. LS acknowledges funding by DFG grant RA 838/5-1. PF is funded by DFG grant SFB/TRR 186 A 04. CR acknowledges funding by BIH grant CRG 2b T1. RNA-seq data are deposited in GEO with accession number GSE93130.

SUPPLEMENTARY MATERIALS

www.sciencemag.org/cgi/content/full/science.aam8526/DC1
Materials and Methods
Figs. S1 to S18
Tables S1 to S7
References (*45*–*64*)

25 January 2017; accepted 26 July 2017
Published online 10 August 2017
10.1126/science.aam8526

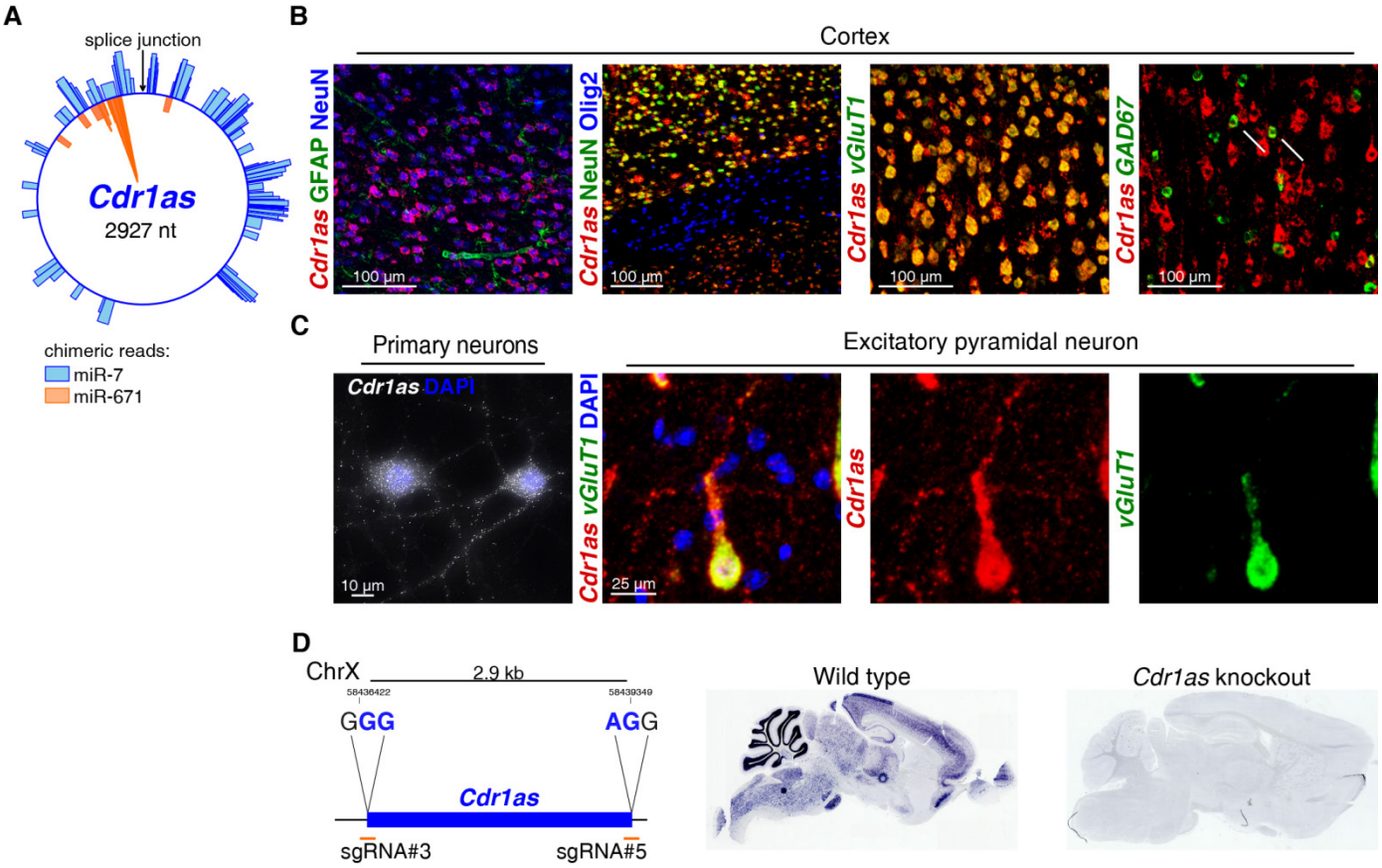

Fig. 1. The circRNA Cdr1as is bound by miR-7 and miR-671, and highly expressed in excitatory neurons. (**A**) Cdr1as is densely bound by Argonaute:miRNA complexes containing miR-7 and miR-671. Bars on the circle represent circRNA:miRNA chimeric reads from Ago2-HITS CLIP data in mouse brain. (**B**) Cdr1as is predominantly expressed in excitatory and less in inhibitory neurons. Marker genes: GFAP - astrocytes, NeuN - neurons, Olig2 - oligodendrocytes vGluT1 - excitatory neurons, GAD67 - inhibitory neurons; arrows mark Cdr1as expression overlap with inhibitory neurons. RNA in situ hybridization in italics, immunostainings in standard font. (**C**) Cdr1as is broadly distributed in neuronal somas and neurites. Left: single molecule fluorescent in situ hybridization for Cdr1as in cultured primary cortical neurons (in vitro day 14), DAPI - nuclear staining. Right: single excitatory pyramidal neuron at lamina II. (**D**) Using CRISPR/Cas9 the *Cdr1as* locus was deleted. The sequences given denote PAMs. Right panel: RNA in situ hybridization confirmed successful genetic ablation of *Cdr1as*.

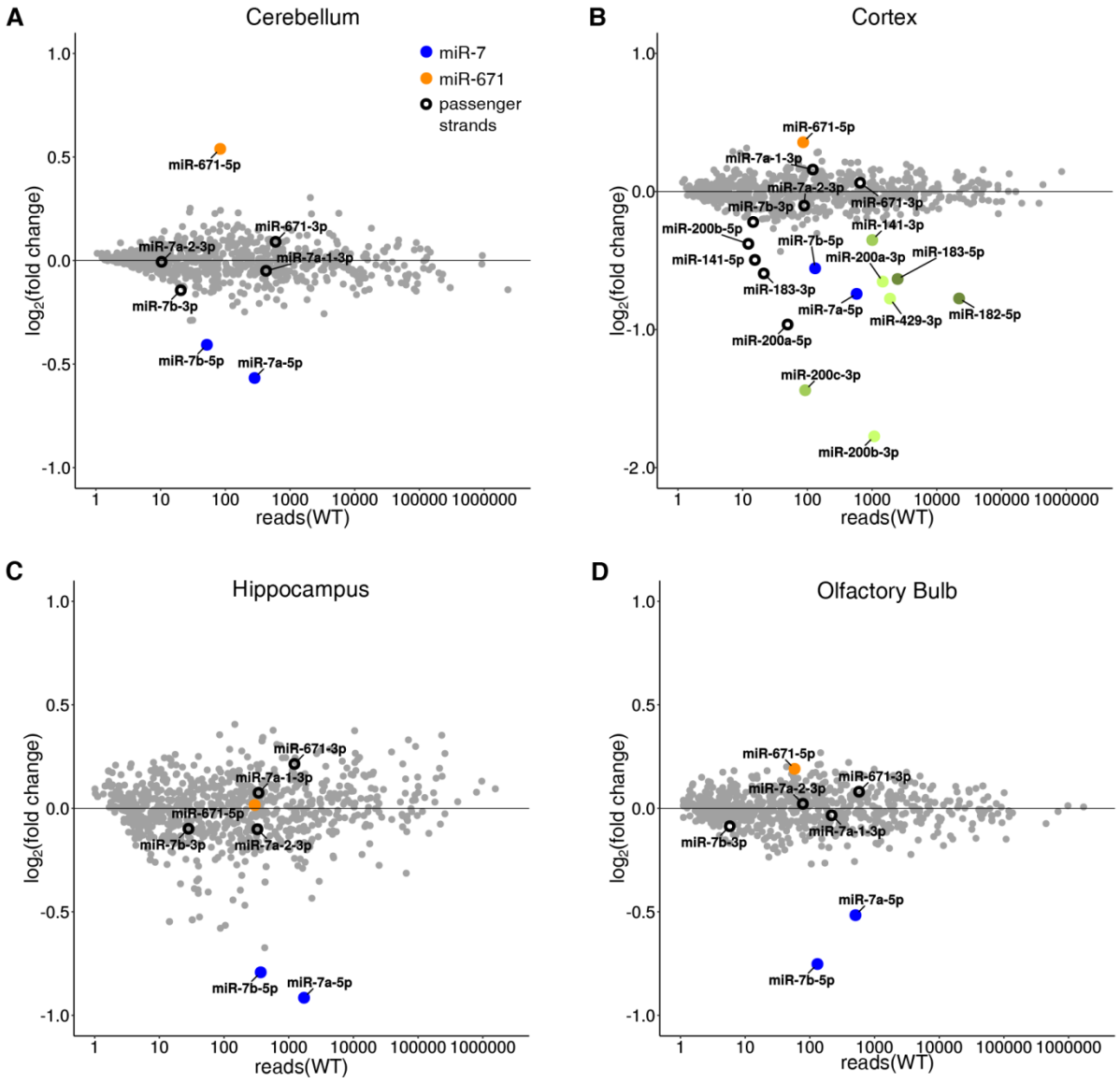

Fig. 2. miRNA expression changes in *Cdr1as* knockout brain regions. Small RNAs were sequenced from mouse (**A**) cerebellum, (**B**) cortex, (**C**) hippocampus and (**D**) olfactory bulb, each in biological replicates $n = 3$, except *Cdr1as* KO hippocampus $n = 2$. Shades of green indicate miRNAs of the same family. Grey – miRNAs with no significant expression change.

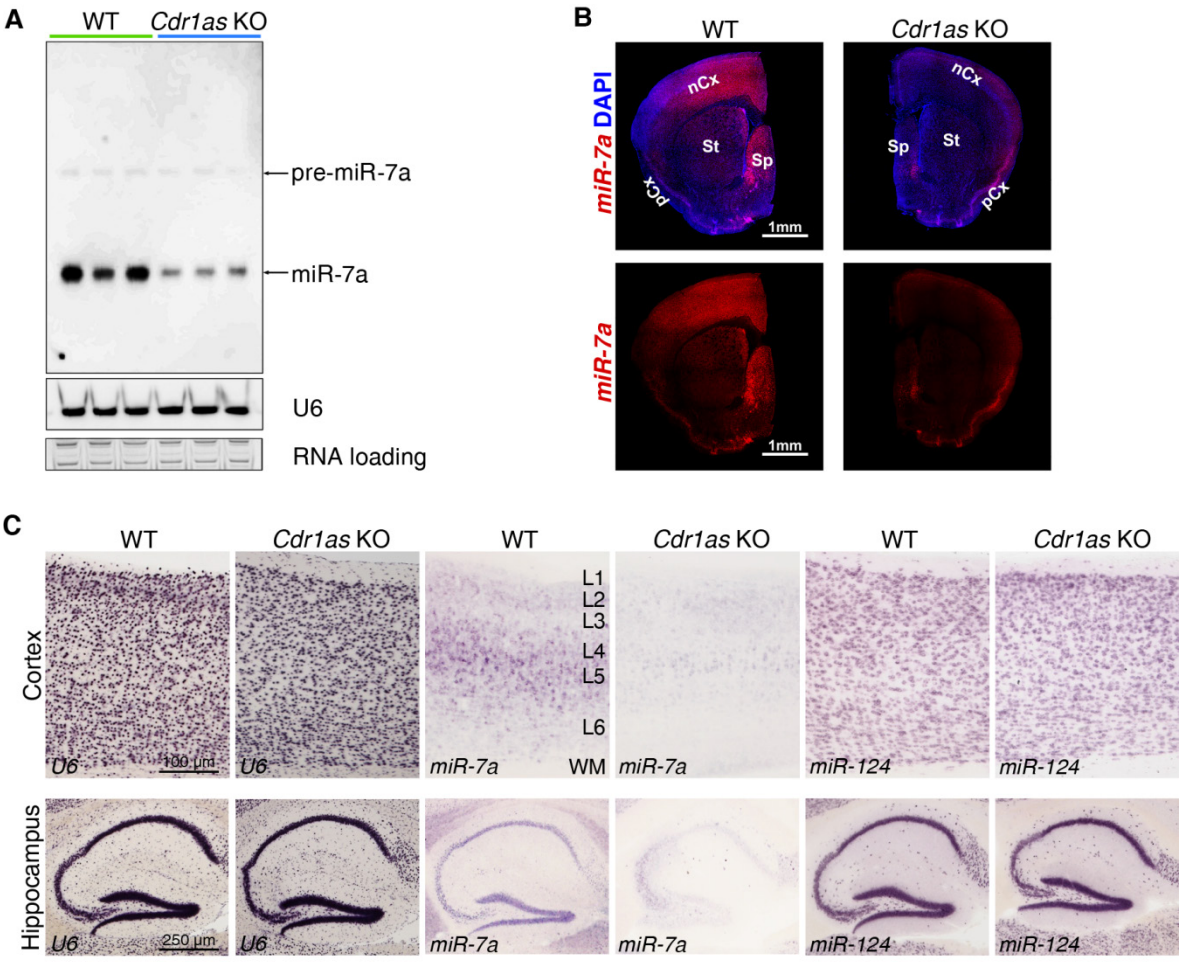

Fig. 3. miR-7a is downregulated in *Cdr1as* knockout brain. miRNA-7a expression in *Cdr1as* KO and WT mouse brain detected using (**A**) Northern blotting, (**B**) fluorescent in situ hybridization and (**C**) chromogenic in situ hybridization. nCx - neocortex, St - striatum, Sp - septum, pCx - piriform cortex, L1-L6 cortical layers, WM - white matter, U6 and miR-124 – control RNAs.

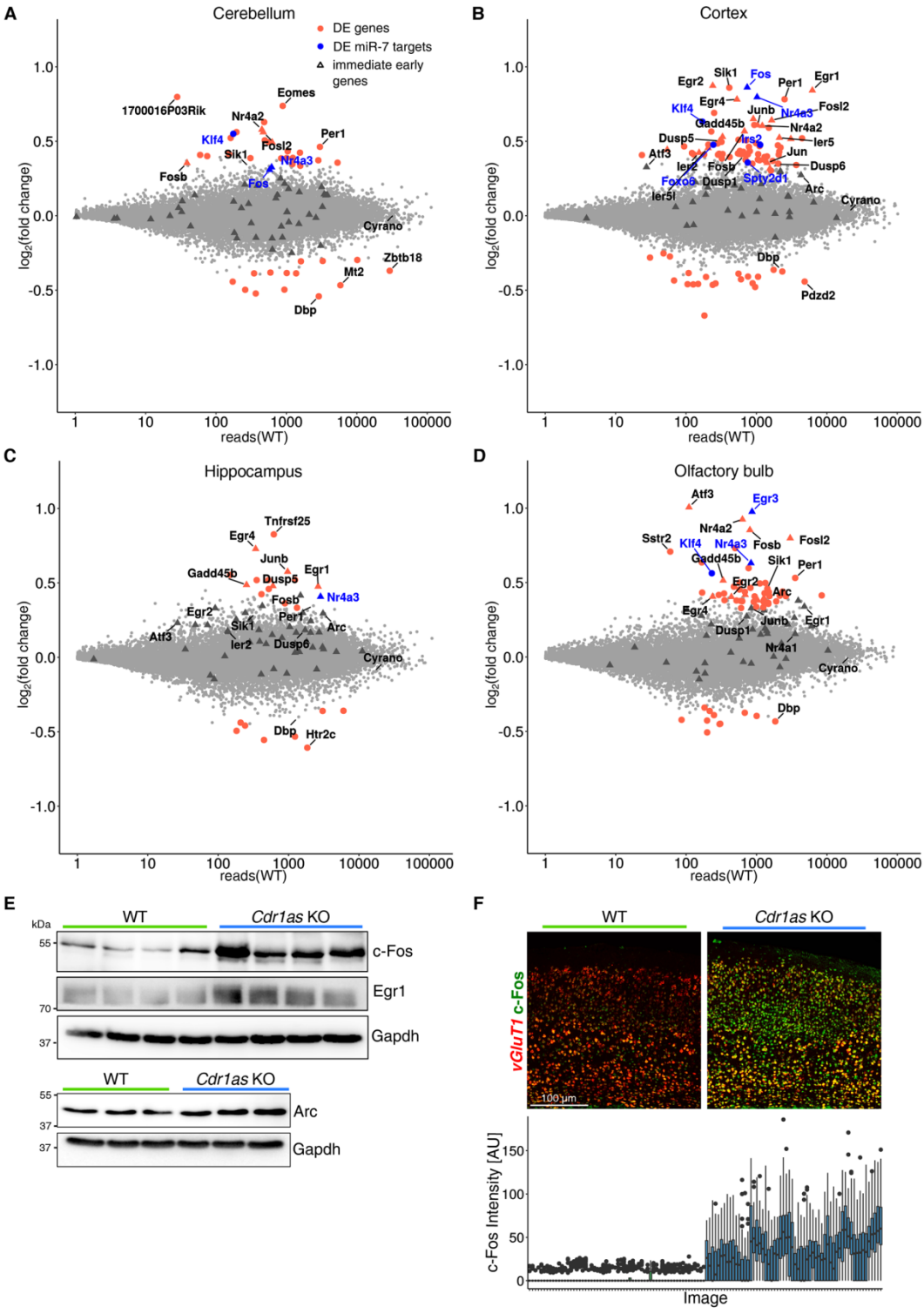

Fig. 4. Gene expression changes in *Cdr1as* knockout brain. Poly(A)-selected RNAs were sequenced from mouse (**A**) cerebellum, (**B**) cortex, (**C**) hippocampus and (**D**) olfactory bulb, each in biological replicates $n = 3$. Red: significantly differentially expressed (DE) genes, blue: significantly DE miR-7 targets, triangles: immediate early genes, grey: no significant expression change. (**E**) Western Blot analysis of differentially expressed immediate early genes in cortical lysates, Gapdh serves as a loading control. (**F**) c-Fos immunohistochemistry combined with in situ hybridization for vGluT1 in somatosensory cortex. Lower panel: c-Fos signal intensity quantification across images ($n = 60$ per genotype).

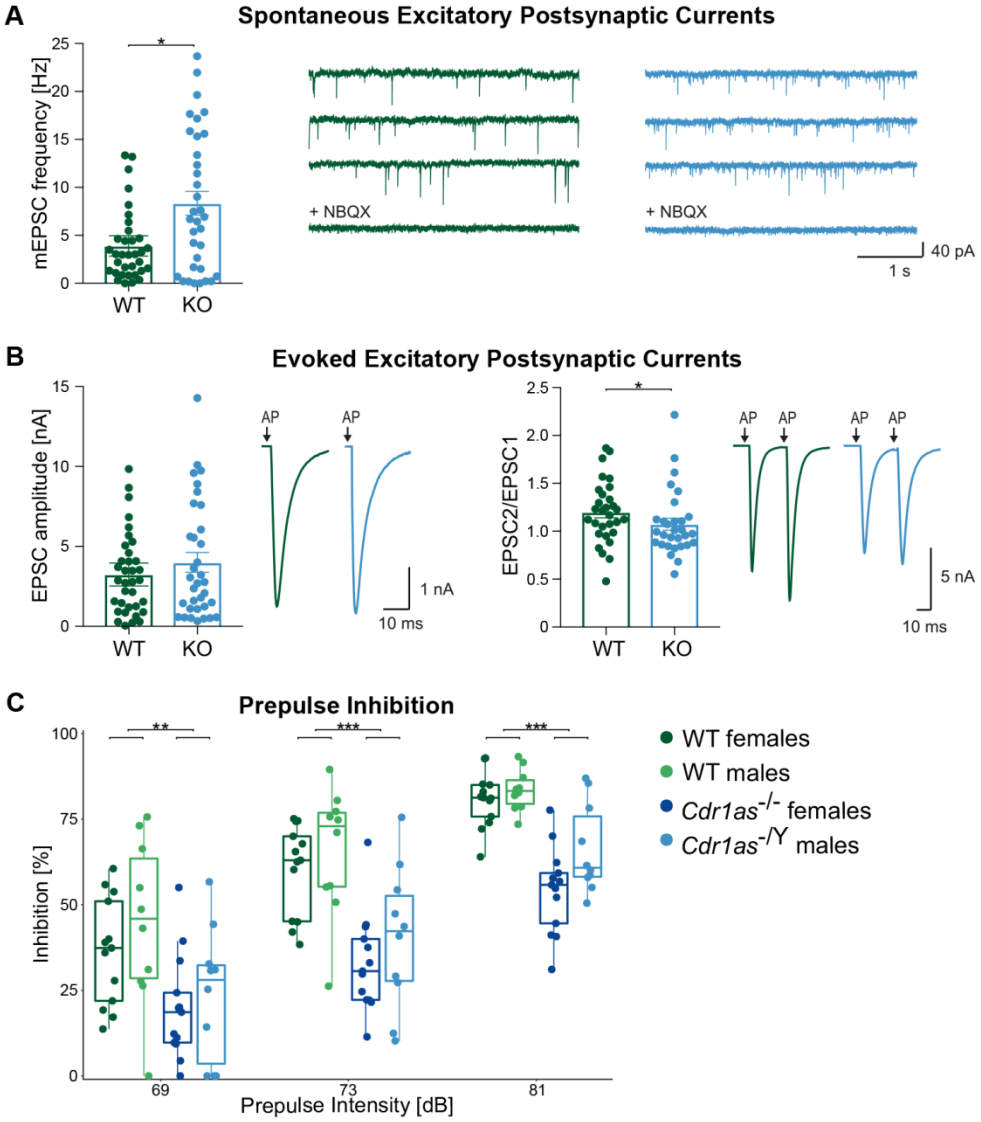

Fig. 5. Loss of *Cdr1as* locus contributes to dysfunctional synaptic neurotransmission and abnormal brain function associated with neuropsychiatric disorders. (**A** and **B**) *Cdr1as* knockout neurons showed an increased spontaneous vesicle release and normal calcium evoked excitatory postsynaptic currents (EPSC). (**A**) Left: mEPSC frequency of WT (n = 34) and *Cdr1as* KO (n = 34) autaptic neurons. Right: representative traces from WT (green) and *Cdr1as* KO (blue) in standard extracellular solution and in AMPA receptor blocking NBQX solution. (**B**) Left: EPSC amplitudes of WT (n = 35) and *Cdr1as* KO (n = 34) neurons. Right: 25 ms inter-stimulus interval paired-pulse ratio of WT (n = 30) and *Cdr1as* KO (n = 30) neurons. Representative traces of evoked EPSCs. Time of action potentials (AP) are indicated by arrows and currents associated with AP induction were blanked to enhance visibility of synaptic current. Mann-Whitney U test was used for statistical analysis, $^{*}P < 0.05$. All data are represented as mean ± SEM. (**C**) *Cdr1as* knockout mice showed deficits in prepulse inhibition (PPI) of a startle reflex. PPI was measured as percentage of the basal startle response. WT females n = 13, *Cdr1as* KO females n = 13, WT males n = 10, *Cdr1as* KO males n = 10. Boxes are defined by the first and third quartiles, median is indicated as a horizontal bar, whiskers span 1.5x inter-quartile range. Three-way ANOVA with Bonferroni-corrected Welch t-test was used for statistical analysis, $^{**}P < 0.01$, $^{***}P < 0.001$. As there was no significant effect of gender, the male and female mice were pooled in post hoc tests.

Loss of a mammalian circular RNA locus causes miRNA deregulation and affects brain function

Monika Piwecka, Petar Glazar, Luis R. Hernandez-Miranda, Sebastian Memczak, Susanne A. Wolf, Agnieszka Rybak-Wolf, Andrei Filipchyk, Filippos Klironomos, Cledi Alicia Cerda Jara, Pascal Fenske, Thorsten Trimbuch, Vera Zywitza, Mireya Plass, Luisa Schreyer, Salah Ayoub, Christine Kocks, Ralf Kühn, Christian Rosenmund, Carmen Birchmeier and Nikolaus Rajewsky

published online August 10, 2017

Science (print ISSN 0036-8075; online ISSN 1095-9203) is published by the American Association for the Advancement of Science, 1200 New York Avenue NW, Washington, DC 20005.